SETD7 controls intestinal regeneration and tumorigenesis by regulating Wnt/β-Catenin and Hippo/YAP signaling

Menno J. Oudhoff[1], Mitchell J.S. Braam[1], Spencer A. Freeman[2], Denise Wong[1], David G. Rattray[1], Jia Wang[2], Frann Antignano[1], Kimberly Snyder[1], Ido Refaeli[1], Michael R. Hughes[1], Kelly M. McNagny[1,7], Michael R. Gold[2], Cheryl H. Arrowsmith[3,4,5], Toshiro Sato[6], Fabio M.V. Rossi[1,7], John Tatlock[8], Dafydd Owen[8], Peter J. Brown[3], Colby Zaph[1,9,10,*]

[1]The Biomedical Research Centre and [2]Department of Microbiology and Immunology,, University of British Columbia, Vancouver, BC, V6T1Z3, Canada; [3]The Structural Genomics Consortium, [4]Princess Margaret Cancer Centre and [5]Department of Medical Biophysics, University of Toronto, Toronto, ON, M5G1L7, Canada; [6]Department of Gastroenterology, School of Medicine, Keio University, Tokyo, 160-8582, Japan; [7]Department of Medical Genetics, University of British Columbia, Vancouver, BC, V6T1Z3, Canada; [8]Worldwide Medicinal Chemistry, Pfizer Worldwide Research and Development, Cambridge, MA 02139, USA; [9]Department of Pathology and Laboratory Medicine, University of British Columbia, Vancouver, BC, V6T1Z3, Canada; [10]Infection and Immunity Program, Monash Biomedicine Discovery Institute and Department of Biochemistry and Molecular Biology, Monash University, Clayton, Victoria, 3800, Australia.

**Corresponding Author, colby.zaph@monash.edu, +61 399050783*

SUMMARY

Intestinal tumorigenesis is a result of mutations in signaling pathways that control cellular proliferation, differentiation, and survival. Mutations in the Wnt/β-Catenin pathway are associated with the majority of intestinal cancers, while dysregulation of the Hippo/Yes-Associated Protein (YAP) pathway is an emerging regulator of intestinal tumorigenesis. In addition, these closely related pathways play a central role during intestinal regeneration. We have previously shown that methylation of the Hippo transducer YAP by the lysine methyltransferase SETD7 controls its subcellular localization and function. We now show that SETD7 is required for Wnt-driven intestinal tumorigenesis and regeneration. Mechanistically, SETD7 is part of a complex containing YAP, AXIN1 and β-Catenin, and SETD7-dependent methylation of YAP facilitates Wnt-induced nuclear accumulation of β-Catenin. Collectively, these results define a methyltransferase-dependent regulatory mechanism that links the Wnt/β-Catenin and Hippo/YAP pathways during intestinal regeneration and tumorigenesis.

INTRODUCTION

Intestinal tumors currently account for approximately 8% of all cancer-related deaths world wide (Stewart and Wild, 2014). Tumorigenesis in the intestine is a complex process that is thought to initiate in intestinal stem cells (ISCs), and requires multiple subsequent mutations in genes that regulate cell growth, differentiation and survival (Barker et al., 2009; Vogelstein et al., 2013). The Wnt/β-Catenin and Hippo/Yes-Associated Protein (YAP) pathways have emerged as regulators of intestinal tumorigenesis. A large proportion of intestinal cancers carry mutations in the Wnt/β-Catenin signaling pathway (Muzny et al., 2012) and deregulation of the Hippo signaling pathway has been associated with a subset of intestinal tumors (Cai et al., 2010; Harvey et al., 2013; Rosenbluh et al., 2012). A better understanding of the cellular and molecular mechanisms regulating these pathways would provide insight into the etiology of intestinal tumorigenesis.

Intestinal homeostasis is regulated by the proliferation and differentiation of a population of 'cycling' intestinal stem cells (ISCs) that express the surface marker LGR5 (Barker et al., 2007). Subsequent studies have identified several other markers for these cells such as ASCL2 and OLFM4, ultimately leading to a 'cycling' ISC signature, which also includes the Hippo transducer YAP (Barker, 2014; Muñoz et al., 2012; van der Flier et al., 2009). In addition, a second type of ISC, which are termed label-retaining cells (LRCs) or reserve stem cells, co-exists with the cycling ISC population (Buczacki et al., 2013; Montgomery et al., 2011; Powell et al., 2012; Sangiorgi and Capecchi, 2008; Takeda et al., 2011; Tetteh et al., 2015; Tian et al., 2011; van Es et al., 2012). LRCs do not participate in the day-to-day turnover of the intestinal epithelium, and are normally destined to become a cell of the secretory lineage (Buczacki et al., 2013; van Es et al., 2012). Interestingly, it has recently been found that enterocyte progenitors can have similar properties as these LRCs (Tetteh et al., 2016). Although the roles of these cell types in homeostasis, regeneration and tumorigenesis are controversial, it is clear that Hippo/YAP and Wnt/β-Catenin signaling are central to the function of intestinal cells *in vivo*.

Several recent studies have demonstrated that the Hippo/YAP and Wnt/β-Catenin pathways are closely related and intimately linked in regulation, structure and function

(Azzolin et al., 2014; 2012; Barry et al., 2013; Byun et al., 2014; Heallen et al., 2011; Imajo et al., 2014; 2012; Rosenbluh et al., 2012; Varelas et al., 2010). However, there have been some conflicting reports concerning the biological and mechanistic function of YAP (or its paralog TAZ) in its role in the Wnt pathway. For example, YAP has been shown to both enhance (Heallen et al., 2011; Rosenbluh et al., 2012) and restrict Wnt signaling (Azzolin et al., 2014; Barry et al., 2013; Imajo et al., 2012; Park et al., 2015; Varelas et al., 2010). Further, knockdown of *Yap* expression in mouse intestinal cells leads to a dramatic decrease in proliferative cells including Wnt-dependent $LGR5^{high}$ ISCs (Imajo et al., 2014), which is in contrast with other reports showing that *Yap* deficiency does not affect intestinal homeostasis but rather is important only during regeneration and tumorigenesis (Azzolin et al., 2014; Barry et al., 2013; Cai et al., 2010; 2015; Gregorieff et al., 2015). These discrepancies can be partially explained by the subcellular localization of these proteins, where cytoplasmic YAP inhibits whereas nuclear YAP promotes Wnt signaling. However, recent reports suggests that nuclear YAP can also inhibit Wnt (Gregorieff et al., 2015; Park et al., 2015). Needless to say, the molecular mechanisms that regulate the interactions between these two pathways have not been fully elucidated.

We have previously reported that SETD7-dependent methylation of YAP mediates its subcellular localization and function *in vitro* and *in vivo* (Barsyte-Lovejoy et al., 2014; Oudhoff et al., 2013). SETD7 is a member of the Suppressor of variegation 3-9-Enhancer of zeste-Trithorax (SET) domain-containing family of lysine methyltransferases, and has been shown to methylate and alter the function of a wide variety of proteins *in vitro* (Herz et al., 2013). The various studies describing interactions between Hippo and Wnt pathways led us to study Wnt-mediated processes in the intestine. We found that SETD7 acts as a facilitator of Wnt-driven tumorigenesis and regeneration. Interestingly, SETD7 is dispensable for normal intestinal homeostasis, but intestinal regeneration is impaired in mice lacking SETD7. Mechanistically, we demonstrate that SETD7 and YAP are associated with the β-Catenin 'destruction complex' and show that SETD7 activity is required for optimal nuclear accumulation of β-Catenin upon activation of the Wnt pathway. These results place SETD7 at the

intersection of the Wnt and Hippo pathways and identify SETD7 as a novel therapeutic target to inhibit intestinal tumorigenesis.

RESULTS

SETD7 is required for optimal tumorigenesis in *Apc*$^{min/+}$ mice

The mouse intestine is a well-established model for studying the Wnt/β-Catenin and Hippo/YAP pathways within the biological contexts of homeostasis, regeneration, and tumorigenesis (Ashton et al., 2010; Azzolin et al., 2014; Barker et al., 2007; Barry et al., 2013; Cai et al., 2015; 2010; Camargo et al., 2007; Gregorieff et al., 2015; Imajo et al., 2014; Metcalfe et al., 2014; Oudhoff et al., 2013; Sansom et al., 2007; Zhou et al., 2011). We have previously found that mice with an intestinal epithelial cell (IEC)-specific deletion of *Setd7* (*Setd7*$^{\Delta IEC}$ mice) had wider and shorter crypts in their large intestines, which was associated with increased IEC turnover, increased nuclear localization of YAP and heightened Hippo/YAP-dependent gene expression (Oudhoff et al., 2013). As nuclear YAP has been reported to enhance Wnt signaling in the heart and in various cancer cell lines (Heallen et al., 2011; Rosenbluh et al., 2012), we wished to test whether SETD7 is involved in intestinal tumorigenesis in a model that relies on Wnt signaling. We therefore crossed *Setd7*$^{-/-}$ mice with *Apc*$^{Min/+}$ mice that spontaneously develop intestinal adenomas due to increased Wnt/β-Catenin activity. We hypothesized that the increased levels of nuclear YAP we observed in *Setd7*$^{\Delta IEC}$ mice would enhance tumorigenesis (Rosenbluh et al., 2012). Surprisingly, *Apc*$^{Min/+}$ mice that lack *Setd7* (*Apc*$^{Min/+}$ *Setd7*$^{-/-}$ mice) had significantly increased lifespans compared to littermate control *Apc*$^{Min/+}$ *Setd7*$^{+/-}$ mice (Figure 1A) with significantly reduced tumor numbers at endpoint that were of similar size (Figures 1B, 1C, S1A and data not shown). Of note, at endpoint most mice were severely anemic, which very likely influenced lifespan.

Treatment of mice with dextran sodium sulfate (DSS) in the drinking water leads to breakdown of the intestinal barrier, inflammatory cell infiltration and transmural damage to the large intestine (Yan et al., 2009), and promotes rapid tumorigenesis in the large intestine of *Apc*$^{Min/+}$ mice (Tanaka et al., 2006). It has been reported that inflammation can induce de-differentiation of non-stem cells to tumor-initiating cells that have stem cell-like properties (Schwitalla et al., 2013), complementing a previous study showing that tumor-initiating cells are LGR5^{high} cycling ISCs (Barker et al., 2009). Although DSS treatment of *Apc*$^{Min/+}$ mice enhanced tumorigenesis in the large intestine, we found that *Apc*$^{Min/+}$ *Setd7*$^{-/-}$ mice developed significantly fewer large intestinal tumors following

DSS treatment (Figure 1D). Thus, SETD7 expression is associated with increased susceptibility to tumorigenesis in the context of dysregulated Wnt signaling.

We analyzed gene expression in small intestinal tumor tissue from aged animals and compared it to adjacent normal tissue (Figure 1E and S1B). We found that both Wnt (*Axin2, Myc, Lgr5*) and Hippo target genes (*Ctgf, Cyr61*) were upregulated in tumor tissue compared to normal tissue (Figure 1E), supporting recent studies showing that mutation in the Wnt/β-Catenin destruction complex components 'activates' YAP and/or TAZ (Azzolin et al., 2014; Cai et al., 2015; Gregorieff et al., 2015). However, activation of Wnt/β-Catenin but not Hippo/YAP target genes was dependent on *Setd7* expression (Figure 1E). Thus, during intestinal tumorigenesis, SETD7 regulates Wnt/β-Catenin-dependent gene expression.

Next, we examined the levels of β-Catenin accumulation and localization in small intestinal tumors (Figures 1F and 1G). Although we found that total amounts of β-Catenin in tumor sections from $Apc^{Min/+}$ $Setd7^{+/-}$ and $Apc^{Min/+}$ $Setd7^{-/-}$ mice were similar, we observed reduced levels of nuclear β-Catenin in tumors from $Apc^{Min/+}$ $Setd7^{-/-}$ mice (Figures 1G), which is consistent with reduced Wnt/β-Catenin-dependent gene expression in these tumors (Figure 1E). We also observed that Wnt-mediated Paneth cell accumulation was diminished in tumors from mice lacking *Setd7* (Figure 1H), further suggesting that SETD7 is important for Wnt-dependent gene expression programs. To directly test if SETD7 activity was an important regulator of Wnt signaling, we derived organoids from tumors of $Apc^{Min/+}$ mice and treated them with the SETD7 inhibitor (*R*)-PFI-2 (Barsyte-Lovejoy et al., 2014). We found that *in vitro* initiation of spheres, as well as Wnt-dependent gene expression (*Lgr5, Axin2,* and *Lyz1*) was reduced upon inhibition of SETD7 (Figures 1I and S1C). Together these results identify a role for SETD7 as a regulator of Wnt/β-Catenin-dependent tumorigenesis in the intestine.

SETD7 is required for Wnt-mediated intestinal regeneration

Given the key role played by stem cells in both tumorigenesis and the response to damage, we employed dextran sulfate sodium (DSS)-induced inflammation to study regeneration in the large intestine. Following a 5-day treatment with DSS, we did not observe any differences between $Setd7^{f/f}$ littermate control mice and $Setd7^{\Delta IEC}$ mice in

acute damage or inflammation as measured by weight loss, reduced colon length, or intestinal inflammation at day 7/8 (Figures 2A, S2A and S2B). Upon returning to regular water, control *Setd7*$^{f/f}$ mice recovered from injury significantly better than *Setd7*$^{\Delta IEC}$ mice as measured by body weight, colon length, inflammatory cytokine production, histology score and number of regenerating crypts at day 15 (Figures 2A-C, S2A-C). Gene expression analysis from IECs isolated from *Setd7*$^{f/f}$ and *Setd7*$^{\Delta IEC}$ mice during regeneration revealed decreased levels of Wnt/β-Catenin-dependent genes *Lgr5* and *Axin2* but no differences in the Notch target gene *Hes1* or Hippo/YAP target *Ctgf* (Figures 2D and S2D). This suggests that SETD7 is required for optimal Wnt/β-Catenin-dependent regeneration following DSS-induced inflammation in the large intestine.

We next assessed regeneration in the small intestine following whole body irradiation, which results in P53-mediated apoptosis of all proliferating IECs, including LGR5^{high} ISCs and, consequently, loss of crypts in the small intestine (Merritt et al., 1994). Following irradiation, the intestine repairs and regenerates itself through a process that requires high levels of Wnt/β-Catenin signaling (Ashton et al., 2010; Barry et al., 2013; Metcalfe et al., 2014). Three days after irradiation, we observed similar ablation of crypts in *Setd7*$^{f/f}$ and *Setd7*$^{\Delta IEC}$ mice (Figures 3A and 3C). However, by day 6 post-irradiation, normal crypt regeneration was observed in *Setd7*$^{f/f}$ mice but not *Setd7*$^{\Delta IEC}$ mice (Figures 3B and 3C). Similar to our results during DSS-induced regeneration, we observed significantly reduced levels of Wnt/β-Catenin target genes *Lgr5* and *Axin2* in IECs isolated from *Setd7*$^{\Delta IEC}$ mice compared to *Setd7*$^{f/f}$ mice during regeneration (Figure 3D). These results identify an important role for SETD7 in Wnt-dependent intestinal regeneration.

Generation of intestinal organoids from crypts isolated from the small intestine of SETD7-deficient mice also identified a role for SETD7 in regulation of intestinal regeneration (Figures 3E-H). We observed that significantly fewer cysts developed from SETD7-deficient crypts compared to heterozygous controls (Figure 3E) despite starting with equivalent numbers of crypt cells (Figure S3A). These cyst-like structures had identical gene expression patterns including low levels of stem cell markers *Lgr5*, *Axin2*, and *Olfm4* (Figures 3G). However, the formation of novel crypts that grow from these cysts was impaired in organoids lacking SETD7 (Figure 3F and S3B). Organoids lacking

SETD7 failed to upregulate the Wnt-dependent genes *Lgr5*, *Axin2*, *Olfm4*, and *Myc* but displayed increased expression of the Hippo/YAP-dependent genes *Ctgf* and *Areg* along with higher expression of the proliferation-associated gene *Mki67* (Figures 3G and S3C). Inhibition of the enzymatic activity of SETD7 with the SETD7 inhibitor (*R*)-PFI-2 during organoid development also resulted in decreased expression of Wnt/β-Catenin-dependent ISC-specific genes *Lgr5*, *Axin2,* and *Ascl2* (Figure 3H). Taken together, these results demonstrate that SETD7 plays a critical role in Wnt/β-Catenin-dependent intestinal processes such as tumorigenesis and regeneration.

SETD7 not required for intestinal homeostasis

During intestinal homeostasis, $LGR5^{high}$ ISCs are constantly replenishing the intestinal epithelium (Barker, 2014; Vermeulen and Snippert, 2014). We found no striking differences in the small intestines of naïve $Setd7^{f/f}$ and $Setd7^{\Delta IEC}$ mice including nuclear β-Catenin in ISCs and Paneth cells at the bottom of crypts (Figure 4A and S4A), or number of goblet cells per villus (Figure S4B). However, we did observe slightly increased numbers of lysozyme-positive Paneth cells per crypt in the $Setd7^{\Delta IEC}$ mice (Figure S4B), which were all normally localized in the bottom of crypts (data not shown). We have previously found differences in crypt width and IEC turnover in the large intestine (Oudhoff et al., 2013). Further, Wnt and Notch target genes (*Lgr5* and *Hes1*) were unaltered whereas Hippo target gene *Ctgf* was expressed significantly higher in IECs isolated from $Setd7^{\Delta IEC}$ mice compared to those from $Setd7^{f/f}$ littermates (Figure 4B), consistent with our previous results in the large intestine (Oudhoff et al., 2013). However, gene expression profiling of all IECs could mask small differences occurring in the stem cell compartment at the bottom of the crypt. We therefore crossed $Setd7^{-/-}$ mice with $Lgr5^{EGFP}$ (*Lgr5-EGFP-IRES-creERT2*) mice, isolated crypts, and analyzed the crypt IECs by flow cytometry for LGR5 (GFP) (Figure 4C). Cycling ISCs are $LGR5^{high}$ and $Setd7^{-/-}$ mice have equal numbers of $LGR5^{high}$ ISCs (Figure 4C). Importantly, these ISCs were equally capable of becoming organoids (Figure 4D), unlike results using whole crypts to generate organoids (Figure 3E). These data show that during homeostasis ISCs do not depend on SETD7 expression, however SETD7 is critical for intestinal regeneration following chemical- or irradiation-induced damage.

SETD7 methyltransferase activity regulates Wnt signaling

Our *in vivo* data suggested that SETD7 is important during regeneration and tumorigenesis, processes that rely on 'high' levels of Wnt signaling. To determine how SETD7 controls Wnt signaling, confluent HEK293 cells were treated with Wnt3A or GSK3 inhibitors (LiCl or CHIR99021) to activate the Wnt/β-Catenin pathway. To block SETD7 activity, cells were either treated with the SETD7 inhibitor (*R*)-PFI-2 or its >500 fold less active enantiomer (*S*)-PFI-2 (Barsyte-Lovejoy et al., 2014), or siRNA constructs were used to knockdown *SETD7*. Activation of the Wnt pathway leads to cytosolic accumulation of β-Catenin, which then translocates to the nucleus to alter gene expression by acting as a transcriptional co-activator (Clevers and Nusse, 2012). We found that accumulation of total β-Catenin upon Wnt activation did not depend on SETD7 or its enzymatic activity (Figures 5A, 5C, S5A, S5C and S6A). In contrast, Wnt-induced *AXIN2* gene expression was abrogated by (*R*)-PFI-2 treatment (Figures 5B and 5D) or by transient knockdown of *SETD7* (Figures S5B and S5D). Consistent with our observations in tumors from $Apc^{Min/+}$ $Setd7^{-/-}$ mice (Figure 1G), we observed that nuclear accumulation of β-Catenin was impaired following inhibition of SETD7 activity (Figures 5E-I and S5E), with a concomitant increase in levels of cytosolic β-Catenin, upon Wnt activation (Figure 5E and 5F). Further, supplementing (*R*)-PFI-2 following Wnt3A treatment did not promote exit of β-Catenin from the nucleus, but rather blocked further nuclear accumulation (Figure 5J), suggesting that SETD7-dependent methylation is required for optimal nuclear localization–but not nuclear retention–of β-Catenin following Wnt activation *in vitro*.

SETD7 mediated control of Wnt signaling requires YAP

To test if the effects of SETD7 on Wnt/β-Catenin signaling were mediated through YAP (Azzolin et al., 2014; Barsyte-Lovejoy et al., 2014; Oudhoff et al., 2013), we analyzed the effects of *SETD7* and *YAP* knockdown on Wnt/β-Catenin pathway activation. Treatment of 293 cells with a pool of 2 siRNAs specific for SETD7, YAP, or both, in the absence of Wnt/β-Catenin pathway activation had no effect on total or cytosolic β-Catenin levels (Figure 6A, S6A and S6B). However, *YAP* knockdown itself did result in a

slight upregulation of *AXIN2* (Figure S6C), consistent with previous reports (Azzolin et al., 2014; Barry et al., 2013; Imajo et al., 2012). LiCl- or CHIR-induced accumulation of β-Catenin protein levels was not affected by knockdown of *SETD7, YAP,* or both (Figure 6A and S6A). Critically, *YAP* knockdown abolished the effects of *SETD7* knockdown on LiCl-induced *AXIN2* expression (Figure 6B), demonstrating that the effects of SETD7 on Wnt/β-Catenin signaling are dependent upon YAP. We further observed that *SETD7* knockdown resulted in increased expression of the YAP target gene *CTGF*, which, predictably, was also dependent on *YAP*, in agreement with our previous studies (Barsyte-Lovejoy et al., 2014; Oudhoff et al., 2013). These results suggest that SETD7-dependent methylation of YAP is an important control point in Wnt-induced β-Catenin function.

SETD7 is in a complex with components of the destruction complex and mediates YAP/β-Catenin interactions

Our results suggest that SETD7 and YAP are critically required for optimal Wnt/β-Catenin mediated gene expression. We next examined whether SETD7 and YAP interacted with components of the destruction complex (Azzolin et al., 2014). We found that SETD7 may be a component of this complex, as immunoprecipitation analyses identified AXIN1 and β-Catenin (Figures 6C and 6D) as binding partners of SETD7 in the absence of Wnt activation. Inhibition of the methyltransferase activity of SETD7 with (*R*)-PFI-2 demonstrated that enzymatic activity is not required for the formation of the SETD7/β-Catenin complex in the absence of Wnt3A (Figures 6D and 6E). However, upon Wnt3A stimulation, the interaction between SETD7 and β-Catenin is lost, and this disassembly is dependent upon SETD7 methyltransferase activity (Figure 6E). Further, we found that the YAP/β-Catenin interaction is dependent on SETD7 methyltransferase activity in the presence or absence of active Wnt signaling (Figure 6F and 6G), suggesting that SETD7-dependent methylation of YAP is critical for stabilizing YAP/β-Catenin interactions irrespective of Wnt signaling (Azzolin et al., 2014; Imajo et al., 2012). In support, we observed that the YAP/AXIN1 interaction depends on the methyltransferase activity of SETD7 (Figure 6H). Importantly, mutation of the methylation site K494 (but not K497) in YAP also blocks YAP-AXIN1 interactions

(Figure 6I). Together, these results identify a role for SETD7 in the cross-regulation of Hippo/YAP and Wnt/β-Catenin signaling by mediating interactions within protein complexes. Our results further suggest that methylation of YAP facilitates accumulation of nuclear β-Catenin upon Wnt activation or GSK3 inhibition.

However, recent studies have shown that YAP-TEAD mediated gene expression may also directly dampen Wnt-dependent gene expression. For example, a recent study showed that abrogation of YAP-TEAD interactions by verteporfin treatment or knockdown of *TEAD* induced Wnt target gene expression (Park et al., 2015). As we observed increased YAP-TEAD activity during intestinal homeostasis (Oudhoff et al., 2013) and in organoids (Figures 3 and 4), we tested whether SETD7 mediates Wnt signaling *via* YAP-TEAD interactions by treating organoids derived from *Setd7*$^{+/-}$ and *Setd7*$^{-/-}$ mice with verteporfin. We found that continuous treatment with verteporfin led to severe growth defects as well as downregulation of *Lgr5*, *Olfm4*, *Axin2* and *Myc* gene expression (Figure 6J and 6K), consistent with results from a different group (Imajo et al., 2014). Critically, the changes in gene expression occurred irrespective of the presence or absence of SETD7, thus supporting our hypothesis that SETD7 does not mediate Wnt signaling by altering YAP-TEAD activity.

SETD7 localization and function is density dependent

As subcellular localization is critical for both Wnt/β-Catenin and Hippo/YAP signaling, we next examined SETD7 localization. We observed that SETD7 localizes to the nucleus in HEK293, Caco-2 and MCF7 cells at low density (sparse), but is found in the cytoplasm and excluded from the nucleus at high cell density (dense) (Figures 7A and 7B). This pattern is strikingly similar to YAP (Figures 7A and S7A), further highlighting that YAP and SETD7 are potentially components of a shared complex. Importantly, we did not observe any effects of SETD7 on Wnt-induced *AXIN2* expression or nuclear β-Catenin accumulation under sparse cell culture conditions in HEK293 and MCF7 cells (Figures 7C, S7B-E) suggesting that cytoplasmic and not nuclear SETD7 regulates Wnt/β-Catenin signaling. Consistent with this, we found that SETD7 is nuclear in cycling ISCs and Paneth cells that regulate intestinal homeostasis, but is cytoplasmic in the rest of the crypt-villus structure (Figure 7D, S7F and S7G). Of note, Yap is absent from

Paneth cells (Gregorieff et al., 2015; Zhou et al., 2011), whereas SETD7 is nuclear. We did observe more Paneth cells in *Setd7*$^{\Delta IEC}$ mice (Figure S4B) suggesting that perhaps SETD7 plays a distinct role in the absence of YAP. In tumors from *Apc*$^{Min/+}$ mice, SETD7 expression was primarily cytoplasmic except for small numbers of cells (Figure 7D), a localization pattern that is similar to LGR5 expression (Barker et al., 2009). Thus, these findings are consistent with a model where nuclear SETD7 in LGR5^{high} ISCs has no effect on Wnt signaling while cytoplasmic SETD7 plays a critical role in potentiating Wnt/β-Catenin signaling through the methylation of YAP, a process required during regeneration and tumorigenesis.

DISCUSSION

In this study, we establish a role for SETD7 in the regulation of Wnt-dependent intestinal tumorigenesis and regeneration. We show that *in vitro* SETD7 is a component of a complex that may contain SETD7, YAP, β-Catenin and AXIN1. Following Wnt stimulation, SETD7-dependent methylation of YAP is required for the dissociation of the complex and nuclear localization of β-Catenin. In the absence of SETD7 or its methyltransferase activity, YAP/β-Catenin interactions are inhibited, β-Catenin fails to translocate to the nucleus and Wnt/β-Catenin-dependent gene expression is abrogated. Thus, our results place SETD7 at the intersection between Hippo/YAP and Wnt/β-Catenin signaling and suggest that methylated YAP is important in the nuclear translocation of β-Catenin, thereby providing a molecular mechanism linking these two pathways.

Several studies have examined the interplay between the Hippo/YAP and Wnt/β-Catenin pathways in intestinal processes, often with contradictory results (Azzolin et al., 2014; Barry et al., 2013; Cai et al., 2015; 2010; Camargo et al., 2007; Gregorieff et al., 2015). For example, two studies show that IEC-intrinsic deletion of *Yap* abolishes intestinal tumorigenesis in $Apc^{Min/+}$ mice (Cai et al., 2015; Gregorieff et al., 2015), whereas others indicate that *Yap* deficiency has negligible effects on tumor formation upon *Apc* deletion in IECs (Azzolin et al., 2014; Barry et al., 2013). Further, it has been shown that both *Yap* deletion and activation, by direct overexpression or by deletion of *Sav,* are detrimental for intestinal regeneration (Barry et al., 2013; Cai et al., 2010). We find that in Wnt-driven tumors there is a significant activation of YAP target genes, in accordance with a recent study (Cai et al., 2015). During 'active' YAP conditions (tumors *in vivo,* low cell density *in vitro*) we do not observe any effects of SETD7 inhibition on YAP function. It has been suggested that YAP may partially drive the development of tumors (Cai et al., 2015; Rosenbluh et al., 2012), explaining why we still observe tumorigenesis in $Apc^{Min/+}/Setd7^{-/-}$ mice. However, Wnt target genes are expressed at significantly lower levels during 'high' Wnt conditions in the intestine (regeneration and tumorigenesis) in mice lacking *Setd7*. Our data is thus in support of a model where 'active' YAP is capable of suppressing Wnt signaling (Gregorieff et al., 2015; Park et al.,

2015), although we propose a mechanism that does not depend on YAP-TEAD-dependent transcription.

Mechanistically, the Wnt/β-Catenin and Hippo/YAP pathways share many similarities. First, activation of both pathways is controlled by regulating the subcellular localization of the effector proteins of each pathway; Wnt signaling results in the nuclear translocation of β-Catenin while activation of the Hippo pathway leads to the cytoplasmic sequestration of YAP. Second, both β-Catenin and YAP have been found to be associated with intercellular junctions through associations with α-catenin and E-cadherin (Huber and Weis, 2001; N. G. Kim et al., 2011; Pokutta and Weis, 2000; Schlegelmilch et al., 2011; Silvis et al., 2011) Furthermore, in addition to sharing general regulatory mechanisms, several studies have identified direct interactions between members of each pathway. For example, YAP has been shown to interact with β-Catenin in the cytoplasm (Imajo et al., 2012) as well as in the nucleus where together they activate tissue-specific gene programs (Heallen et al., 2011; Rosenbluh et al., 2012). In addition, YAP has also been found to interact with Wnt pathway members Dishevelled and AXIN1 (Azzolin et al., 2014; Barry et al., 2013; Varelas et al., 2010). Taken together, these studies suggest that the Wnt/β-Catenin and Hippo/YAP pathways may be part of a larger pathway that integrates these signals in tissues. Our results identify SETD7 as a novel member of this Wnt/Hippo 'super-pathway' through methylation of YAP. Azzolin *et al.* specifically describe that YAP affects the destruction complex by recruiting β-TrCP to AXIN1, thereby controlling β-Catenin protein levels (Azzolin et al., 2014). We fail to observe SETD7 or YAP-mediated control of total β-Catenin protein levels with or without Wnt signaling, even though the YAP-AXIN1 interaction is mediated by methylation. Based on our data we would propose a mechanism in which the continuous cytoplasmic-nuclear shuttling of YAP, and destruction complex members such as APC and AXIN1 (Cong and Varmus, 2004; Dupont et al., 2011; Henderson, 2000; Schmitz et al., 2013) is required for optimal nuclear accumulation of β-Catenin. Further, it has also been proposed that YAP may be phosphorylated and retained in the nucleus (Li et al., 2014; Wada et al., 2011), leading us to speculate that methylation and phosphorylation are involved in a complex interplay to establish protein complexes important for the localization and shuttling of β-Catenin and YAP.

Our studies also highlight the important role of methylation as a post-translational modification (PTM) that can modulate signaling output. Thus, in addition to established PTMs such as phosphorylation and ubiquitination, we propose that methylation of non-histone proteins is an important regulator of signal transduction, which is in line with several recent studies (Fang et al., 2014; E. Kim et al., 2013; Mazur et al., 2014). Indeed, a recent study identified a role for SETD7 in the direct methylation of β-Catenin (Shen et al., 2015). It was proposed that SETD7-dependent methylation of β-Catenin was required for optimal degradation in response to oxidative conditions. We fail to find any evidence of direct methylation of β-Catenin by SETD7 following canonical activation of Wnt signaling. Further, we do not observe any changes in the levels of β-Catenin in the absence of SETD7, suggesting that degradation is not directly affected by SETD7 deficiency. Thus, although our results do not excludes the possibility that β-Catenin is methylated, it is likely that SETD7 is not the relevant methyltransferase. Instead, our results point to an indirect role for SETD7 through its methylation of YAP in the control of Wnt/β-Catenin signaling.

Dynamic responsiveness of signal transduction pathways to exogenous signals will require the ability to rapidly remove methylation marks. The identification and analysis of the demethylase(s) involved in this pathway will provide additional therapeutic targets to modulate Wnt/Hippo-dependent physiological processes. Indeed, a recent study has identified a demethylase that is important for Wnt-induced nuclear stabilization of β-Catenin (Lu et al., 2015). Although this study supports our findings that methylation is a critical component of Wnt signaling, it is likely that distinct mechanisms are in play. For example, Lu *et al.* finds that degradation of nuclear β-Catenin is specifically affected, while we do not detect any differences in β-Catenin levels. In addition, the authors show that β-Catenin itself is methylated using an antibody specifically recognizing di-methylated lysines. As SETD7 is a mono-methylase, our findings do not support that SETD7 is the methylase in this case. Nevertheless, this indicates that methylation is important at several levels in the Wnt signaling pathway.

In summary, we have shown that SETD7-dependent methylation of YAP is a critical central regulatory mechanism that links the Wnt/β-Catenin and Hippo/YAP

pathways. The results of these studies have important ramifications for the treatment of intestinal tumors and provide a new pathway to target for the development of novel therapeutics.

MATERIAL AND METHODS

Cell culture

HEK293, MCF7, and Caco-2 cell lines were grown in DMEM supplemented with 10% FCS and antibiotics. Wnt3A (PeproTech or R&D systems) was used at 100 ng/ml, LiCl (a kind gift from Le Su) at 20 mM, CHIR-99021 (StemCell Technologies) at 3 μM, (*S*)-PFI-2 and (*R*)-PFI-2 between 1 and 10 μM was commonly added 30 minutes before the start of Wnt stimulation, unless otherwise noted (Figure 5J). Transient knockdown of gene expression was performed using siRNA (Silencer Select (*SETD7* S37451/S37452, *YAP* S20366/S20367, Negative Control No.1), Life Technologies), transfected with Lipofectamine RNAiMAX (Life Technologies) according to manufacturer.

Cell lysis, immunoprecipitation (IP) and immunoblotting (IB)

Cells were lysed using whole cell lysate extraction (WCE) buffer (1% NP40 in TBS, 0.02% SDS, with protease inhibitor cocktail without EDTA (Roche)). Cytosolic/nuclear fractionation was done using cytosolic buffer (0.33 M Sucrose, 10 mM HEPES, 1 mM $MgCl_2$, 0.1 % Triton X100) for 10 min., spin down 2,400 RPM for 5 min., supernatant was used as cytosolic fraction. Nuclear fraction was obtained by dissolving pellet in 'membrane buffer' (0.25 M Sucrose, 20 mM HEPES, 10 mM KCl, 1.5 mM $MgCl_2$, 1 mM EDTA) for 25 minutes on ice, this is to get rid of as much membranous β-Catenin as possible. This was spun down at 3,000 RPM for 5 min. and the pellet was considered the nuclear fraction, which was dissolved in sample buffer containing 10% glycerol and 0.1 % SDS. Or fractionation was done using a fractionation kit (Millipore) according to the manufacturer (Figure S5E). Immunoprecipitation was done in WCE using anti-MYC (9E10, Ablab), anti-SETD7 (Abcam), anti-YAP (Cell Signaling Technologies/Santa Cruz), anti-β-Catenin (Santa Cruz) or anti-FLAG (M2, Sigma) antibodies for 2 h at 4 degrees, then Prot. A/G slurry (Santa Cruz) for 2 hours, washed 4 times in WCE. Antibodies for western blotting: anti-β-Catenin, anti-YAP/TAZ (Santa Cruz), anti-SETD7, anti-Histone 3 (Abcam), anti-AXIN1, anti-$pYAP^{S127}$ (Cell Signaling Technologies). HEK293 cells were transfected at 80 % confluency using Lipofectamine 3000 (Life Technologies) using MYC-AXIN1 (Addgene '21287'(Zeng et al., 1997)),

YAP^{K494R}, YAP^{K497R}, YAP^{2KR}, and HA-SETD7 as published (Hata et al., 2012; Lehnertz et al., 2011; Oudhoff et al., 2013).

Confocal imaging and quantification

HEK293 cells were seeded onto fibronectin (Sigma F1141, used at 10 ug/mL) coated 8 well chamber slides (ibidi) overnight. Cells were washed with PBS before addition of (*S*)-PFI-2 or (*R*)-PFI-2 compounds (1 μM) in empty DMEM media or Wnt3A (100 ng/ml). Subsequently, compounds or Wnt3a were added at indicated times. Cells were fixed with 4% PFA in PBS, permeabilized with 1% Triton-X, blocked in 5% BSA, and stained. Anti-β-Catenin (610153, BD Biosciences) was used at 1:400, Alexa488 anti-mouse was used at 1:200. ProLong Gold mounting media with DAPI was added before imaging. Quantification of nuclear β-Catenin was performed using ImagePro where masks for individual nuclei were drawn using the DAPI signal and the β-Catenin signal within these masks was determined as nuclear β-Catenin. This was performed for 3-5 fields from 3 experiments. Caco-2 and MCF7 cells were seeded directly on chamber slides (ibidi), at low or high density, and stained using anti-SETD7 1:400 (2D10, Abcam) anti-YAP 1:5000 (a kind gift from Dr. Sudol).

Mice and Regeneration Models

Villin-Cre, *Lgr5-EGFP-IRES*-creERT2, and *Apc*$^{Min/+}$ (C57BL/6 background) mice were obtained from Jackson Laboratories. *Setd7*$^{-/-}$ and *Setd7*$^{f/f}$ mice were described previously (Lehnertz et al., 2011; Oudhoff et al., 2013). We did not observe any physiological effects from Cre expression. Animals were maintained in a specific-pathogen-free environment and tested negative for pathogens in routine screening. All experiments were carried out at the University of British Columbia following institutional guidelines. Mice were given 3.5% Dextran Sodium Sulfate (DSS) (MW 36,000-50,000, MP Biomedicals) in their drinking water *ad libitum* for 5 days, after which this was replaced by normal water. Body weights were assessed daily, as well as their stool (for diarrhea and blood) and general clinical symptoms of distress. Mice were euthanized at days 7, 8, and 15 to study regeneration.

Mice were lethally irradiated (10-12 Gy) and small intestinal repair was assessed at day 3 and day 6/7.

Tissue Staining

Tissues were fixed in formalin and paraffin-embedded. Sections (5 μm) were stained with hematoxylin and eosin (H&E) or Periodic acid-Schiff (PAS). For immunohistochemistry anti-β-Catenin (BD biosciences), anti-Setd7 (Abcam, 2D10), anti-GFP (Abcam, ab13790), anti-Lysozyme (DAKO), anti-Ki67 (ThermoScientific) antibodies were used and HRP-conjugated antibody was used in combination with peroxidase substrate kit (DAB) (Vector Laboratories).

Crypt isolation, IEC preparation, and organoid culture

Crypt isolation, IEC preparation, and organoid culture was performed as described (Sato and Clevers, 2013; Sato et al., 2009). For flow cytometry, we gated live (DAPI negative) crypt IECs. BD Matrigel Matrix Growth Factor Reduced (BD Biosciences), EGF (Life Technologies), Noggin (PeproTech), and R-Spondin (PeproTech) were used at recommended concentrations (Sato and Clevers, 2013). Apc^{Min} derived organoids were grown in EGF and Noggin without R-Spondin. Organoids grown from $Lgr5^{high}$ sorted cell was done using Intesticult (StemCell Technologies), which was also used for the verteporfin (Visudyne was a kind gift from Novartis) treatments (3 μM, changed daily). In cultures using (*R*)-PFI-2 (1 μM), the compound was supplemented every 8 h, and medium was refreshed every 24 h.

Mesenteric lymph node cell re-stimulation and ELISA

Mesenteric lymph node cells from DSS-treated mice were isolated and single-cell suspensions were plated at 3–4 × 10^6 per ml in the medium or in the presence of antibodies against CD3 (145-2C11) and CD28 (37.51; 1 μg ml^{-1} each; eBioscience, San Diego, CA) for 72 h. Cytokine production from cell-free supernatants was determined by standard sandwich enzyme-linked immunosorbent assay (ELISA) using commercially available antibodies (eBioscience).

RNA extraction and qPCR

RNA was purified from whole intestine using mechanical disruption followed by TRIzol according to the manufacturer's instructions, or from IECs or cultured cells using RNeasy isolation kit (Qiagen). Reverse transcription using High Capacity cDNA Reverse Transcription kit (Applied Biosystems) was used to generate cDNA and qPCR was performed using SYBR green with primers from the Primer Bank (http://pga.mgh.harvard.edu/primerbank) using SYBR green chemistry on an ABI 7900 real-time PCR system (Applied Biosystems). Samples were normalized against *Actb* or *Gapdh* and are presented as fold over 'wild type' or relative to housekeeping gene as is indicated in figure legends.

Statistical analysis

Results are presented as mean±s.e.m. Statistical significance was determined either using Student's *t* test or 1-way ANOVA with post hoc tests, or, when n<10 non-parametric testing (Mann Whitney test) was done. Results with *P* values <0.05 were considered significant.

AUTHOR CONTRIBUTIONS

M.J.O, S.A.F., D.W., M.J.S.B., D.G.R., J. W., K.S., M.R.H., M.R.G., K.M.M., I.R., F.M.V.R., T.S. and C.Z. designed and performed the research and/or provided advice and technical expertise. C.H.A, P.J.B., D.O. and F.M.V.R. provided unique reagents. M.J.O. and C.Z. analyzed the data and wrote the manuscript.

ACKNOWLEDGEMENTS

This work was supported by the Canadian Institutes of Health Research (to M.R.G., K.M.M and C.Z.) and a Canada Foundation for Innovation grant (to C.Z.). The development of the mouse strains used in this study was supported by funds from the Leon Judah Blackmore Foundation (to F.M.V.R.). S.A.F. was supported by fellowships from the CIHR and the Michael Smith Foundation for Health Research (MSFHR). M.J.O. is a Banting Fellow and a MSFHR Fellow. F.M.V.R. is a Distinguished Scholar in Residence of the Peter Wall Institute for Advanced Studies. C.Z. is a MSFHR Career Investigator and a veski innovation fellow. The authors declare there are no competing financial interests.

REFERENCES

Ashton, G.H., Morton, J.P., Myant, K., Phesse, T.J., Ridgway, R.A., Marsh, V., Wilkins, J.A., Athineos, D., Muncan, V., Kemp, R., Neufeld, K., Clevers, H., Brunton, V., Winton, D.J., Wang, X., Sears, R.C., Clarke, A.R., Frame, M.C., Sansom, O.J., 2010. Focal adhesion kinase is required for intestinal regeneration and tumorigenesis downstream of Wnt/c-Myc signaling. Dev Cell 19, 259–269. doi:10.1016/j.devcel.2010.07.015

Azzolin, L., Panciera, T., Soligo, S., Enzo, E., Bicciato, S., Dupont, S., Bresolin, S., Frasson, C., Basso, G., Guzzardo, V., Fassina, A., Cordenonsi, M., Piccolo, S., 2014. YAP/TAZ Incorporation in the β-Catenin Destruction Complex Orchestrates the Wnt Response. Cell 158, 157–170. doi:10.1016/j.cell.2014.06.013

Azzolin, L., Zanconato, F., Bresolin, S., Forcato, M., Basso, G., Bicciato, S., Cordenonsi, M., Piccolo, S., 2012. Role of TAZ as mediator of Wnt signaling. Cell 151, 1443–1456. doi:10.1016/j.cell.2012.11.027

Barker, N., 2014. Adult intestinal stem cells: critical drivers of epithelial homeostasis and regeneration. Nat Rev Mol Cell Biol 15, 19–33. doi:10.1038/nrm3721

Barker, N., Ridgway, R.A., van Es, J.H., van de Wetering, M., Begthel, H., van den Born, M., Danenberg, E., Clarke, A.R., Sansom, O.J., Clevers, H., 2009. Crypt stem cells as the cells-of-origin of intestinal cancer. Nature 457, 608–611. doi:10.1038/nature07602

Barker, N., van Es, J.H., Kuipers, J., Kujala, P., van den Born, M., Cozijnsen, M., Haegebarth, A., Korving, J., Begthel, H., Peters, P.J., Clevers, H., 2007. Identification of stem cells in small intestine and colon by marker gene Lgr5. Nature 449, 1003–1007. doi:10.1038/nature06196

Barry, E.R., Morikawa, T., Butler, B.L., Shrestha, K., la Rosa, de, R., Yan, K.S., Fuchs, C.S., Magness, S.T., Smits, R., Ogino, S., Kuo, C.J., Camargo, F.D., 2013. Restriction of intestinal stem cell expansion and the regenerative response by YAP. Nature 493, 106–110. doi:10.1038/nature11693

Barsyte-Lovejoy, D., Li, F., Oudhoff, M.J., Tatlock, J.H., Dong, A., Zeng, H., Wu, H., Freeman, S.A., Schapira, M., Senisterra, G.A., Kuznetsova, E., Marcellus, R., Allali-Hassani, A., Kennedy, S., Lambert, J.-P., Couzens, A.L., Aman, A., Gingras, A.-C., Al-Awar, R., Fish, P.V., Gerstenberger, B.S., Roberts, L., Benn, C.L., Grimley, R.L., Braam, M.J.S., Rossi, F.M.V., Sudol, M., Brown, P.J., Bunnage, M.E., Owen, D.R., Zaph, C., Vedadi, M., Arrowsmith, C.H., 2014. (R)-PFI-2 is a potent and selective inhibitor of SETD7 methyltransferase activity in cells. Proc Natl Acad Sci U S A 111, 12853–12858. doi:10.1073/pnas.1407358111

Buczacki, S.J.A., Zecchini, H.I., Nicholson, A.M., Russell, R., Vermeulen, L., Kemp, R., Winton, D.J., 2013. Intestinal label-retaining cells are secretory precursors expressing Lgr5. Nature 495, 65–69. doi:10.1038/nature11965

Byun, M.R., Hwang, J.-H., Kim, A.R., Kim, K.M., Hwang, E.S., Yaffe, M.B., Hong, J.-H., 2014. Canonical Wnt signalling activates TAZ through PP1A during osteogenic differentiation. Cell Death Differ. 21, 854–863. doi:10.1038/cdd.2014.8

Cai, J., Maitra, A., Anders, R.A., Taketo, M.M., Pan, D., 2015. β-Catenin destruction complex-independent regulation of Hippo-YAP signaling by APC in intestinal tumorigenesis. Genes Dev 29, 1493–1506. doi:10.1101/gad.264515.115

Cai, J., Zhang, N., Zheng, Y., de Wilde, R.F., Maitra, A., Pan, D., 2010. The Hippo

signaling pathway restricts the oncogenic potential of an intestinal regeneration program. Genes Dev. 24, 2383–2388. doi:10.1101/gad.1978810
Camargo, F.D., Gokhale, S., Johnnidis, J.B., Fu, D., Bell, G.W., Jaenisch, R., Brummelkamp, T.R., 2007. YAP1 increases organ size and expands undifferentiated progenitor cells. Curr Biol 17, 2054–2060. doi:10.1016/j.cub.2007.10.039
Clevers, H., Nusse, R., 2012. Wnt/β-catenin signaling and disease. Cell 149, 1192–1205. doi:10.1016/j.cell.2012.05.012
Cong, F., Varmus, H., 2004. Nuclear-cytoplasmic shuttling of Axin regulates subcellular localization of -catenin. PNAS 101, 2882–2887. doi:10.1073/pnas.0307344101
Dupont, S., Morsut, L., Aragona, M., Enzo, E., Giulitti, S., Cordenonsi, M., Zanconato, F., Le Digabel, J., Forcato, M., Bicciato, S., Elvassore, N., Piccolo, S., 2011. Role of YAP/TAZ in mechanotransduction. Nature 474, 179–183. doi:10.1038/nature10137
Fang, L., Zhang, L., Wei, W., Jin, X., Wang, P., Tong, Y., Li, J., Du, J.X., Wong, J., 2014. A Methylation-Phosphorylation Switch Determines Sox2 Stability and Function in ESC Maintenance or Differentiation. Mol Cell 55, 537–551. doi:10.1016/j.molcel.2014.06.018
Gregorieff, A., Liu, Y., Inanlou, M.R., Khomchuk, Y., Wrana, J.L., 2015. Yap-dependent reprogramming of Lgr5(+) stem cells drives intestinal regeneration and cancer. Nature 526, 715–718. doi:10.1038/nature15382
Harvey, K.F., Zhang, X., Thomas, D.M., 2013. The Hippo pathway and human cancer. Nature reviews. Cancer 13, 246–257. doi:10.1038/nrc3458
Hata, S., Hirayama, J., Kajiho, H., Nakagawa, K., Hata, Y., Katada, T., Furutani-Seiki, M., Nishina, H., 2012. A novel acetylation cycle of transcription co-activator Yes-associated protein that is downstream of Hippo pathway is triggered in response to SN2 alkylating agents. J Biol Chem 287, 22089–22098. doi:10.1074/jbc.M111.334714
Heallen, T., Zhang, M., Wang, J., Bonilla-Claudio, M., Klysik, E., Johnson, R.L., Martin, J.F., 2011. Hippo pathway inhibits Wnt signaling to restrain cardiomyocyte proliferation and heart size. Science 332, 458–461. doi:10.1126/science.1199010
Henderson, B.R., 2000. Nuclear-cytoplasmic shuttling of APC regulates beta-catenin subcellular localization and turnover. Nat Cell Biol 2, 653–660. doi:10.1038/35023605
Herz, H.-M., Garruss, A., Shilatifard, A., 2013. SET for life: biochemical activities and biological functions of SET domain-containing proteins. Trends Biochem. Sci. 38, 621–639. doi:10.1016/j.tibs.2013.09.004
Huber, A.H., Weis, W.I., 2001. The Structure of the β-Catenin/E-Cadherin Complex and the Molecular Basis of Diverse Ligand Recognition by β-Catenin. Cell 105, 391–402. doi:10.1016/S0092-8674(01)00330-0
Imajo, M., Ebisuya, M., Nishida, E., 2014. Dual role of YAP and TAZ in renewal of the intestinal epithelium. Nat Cell Biol 17, 7–19. doi:10.1038/ncb3084
Imajo, M., Miyatake, K., Iimura, A., Miyamoto, A., Nishida, E., 2012. A molecular mechanism that links Hippo signalling to the inhibition of Wnt/β-catenin signalling. Embo J 31, 1109–1122. doi:10.1038/emboj.2011.487
Kim, E., Kim, M., Woo, D.-H., Shin, Y., Shin, J., Chang, N., Oh, Y.T., Kim, H., Rheey, J., Nakano, I., Lee, C., Joo, K.M., Rich, J.N., Nam, D.-H., Lee, J., 2013. Phosphorylation of EZH2 activates STAT3 signaling via STAT3 methylation and promotes tumorigenicity of glioblastoma stem-like cells. Cancer Cell 23, 839–852.

doi:10.1016/j.ccr.2013.04.008
Kim, N.G., Koh, E., Chen, X., Gumbiner, B.M., 2011. E-cadherin mediates contact inhibition of proliferation through Hippo signaling-pathway components. Proc Natl Acad Sci U S A 108, 11930–11935. doi:10.1073/pnas.1103345108
Lehnertz, B., Rogalski, J.C., Schulze, F.M., Yi, L., Lin, S., Kast, J., Rossi, F.M., 2011. p53-Dependent Transcription and Tumor Suppression Are Not Affected in Set7/9-Deficient Mice. Mol Cell 43, 673–680. doi:10.1016/j.molcel.2011.08.006
Li, W., Cooper, J., Zhou, L., Yang, C., Erdjument-Bromage, H., Zagzag, D., Snuderl, M., Ladanyi, M., Hanemann, C.O., Zhou, P., Karajannis, M.A., Giancotti, F.G., 2014. Merlin/NF2 Loss-Driven Tumorigenesis Linked to CRL4DCAF1-Mediated Inhibition of the Hippo Pathway Kinases Lats1 and 2 in the Nucleus. Cancer Cell 26, 48–60. doi:10.1016/j.ccr.2014.05.001
Lu, L., Gao, Y., Zhang, Z., Cao, Q., Zhang, X., Zou, J., Cao, Y., 2015. Kdm2a/b Lysine Demethylases Regulate Canonical Wnt Signaling by Modulating the Stability of Nuclear β-Catenin. Dev Cell 33, 660–674. doi:10.1016/j.devcel.2015.04.006
Mazur, P.K., Reynoird, N., Khatri, P., Jansen, P.W.T.C., Wilkinson, A.W., Liu, S., Barbash, O., Van Aller, G.S., Huddleston, M., Dhanak, D., Tummino, P.J., Kruger, R.G., Garcia, B.A., Butte, A.J., Vermeulen, M., Sage, J., Gozani, O., 2014. SMYD3 links lysine methylation of MAP3K2 to Ras-driven cancer. Nature 510, 283–. doi:10.1038/nature13320
Merritt, A.J., Potten, C.S., Kemp, C.J., Hickman, J.A., Balmain, A., Lane, D.P., Hall, P.A., 1994. The role of p53 in spontaneous and radiation-induced apoptosis in the gastrointestinal tract of normal and p53-deficient mice. Cancer Res 54, 614–617.
Metcalfe, C., Kljavin, N.M., Ybarra, R., de Sauvage, F.J., 2014. Lgr5+ stem cells are indispensable for radiation-induced intestinal regeneration. Cell Stem Cell 14, 149–159. doi:10.1016/j.stem.2013.11.008
Montgomery, R.K., Carlone, D.L., Richmond, C.A., Farilla, L., Kranendonk, M.E.G., Henderson, D.E., Baffour-Awuah, N.Y., Ambruzs, D.M., Fogli, L.K., Algra, S., Breault, D.T., 2011. Mouse telomerase reverse transcriptase (mTert) expression marks slowly cycling intestinal stem cells. Proc Natl Acad Sci U S A 108, 179–184. doi:10.1073/pnas.1013004108
Muñoz, J., Stange, D.E., Schepers, A.G., van de Wetering, M., Koo, B.-K., Itzkovitz, S., Volckmann, R., Kung, K.S., Koster, J., Radulescu, S., Myant, K., Versteeg, R., Sansom, O.J., van Es, J.H., Barker, N., van Oudenaarden, A., Mohammed, S., Heck, A.J.R., Clevers, H., 2012. The Lgr5 intestinal stem cell signature: robust expression of proposed quiescent “+4” cell markers. Embo J 31, 3079–3091. doi:10.1038/emboj.2012.166
Muzny, D.M., Bainbridge, M.N., Chang, K., Dinh, H.H., Drummond, J.A., Fowler, G., Kovar, C.L., Lewis, L.R., Morgan, M.B., Newsham, I.F., Reid, J.G., Santibanez, J., Shinbrot, E., Trevino, L.R., Wu, Y.-Q., Wang, M., Gunaratne, P., Donehower, L.A., Creighton, C.J., Wheeler, D.A., Gibbs, R.A., Voet, D., Cibulskis, K., Stojanov, P., McKenna, A., Lander, E.S., Gabriel, S., Ding, L., Fulton, R.S., Koboldt, D.C., Wylie, T., Walker, J., Dooling, D.J., Fulton, L., Delehaunty, K.D., Fronick, C.C., Demeter, R., Mardis, E.R., Wilson, R.K., Chu, A., Chun, H.-J.E., Mungall, A.J., Pleasance, E., Gordon Robertson, A., Stoll, D., Balasundaram, M., Birol, I., Butterfield, Y.S.N., Chuah, E., Coope, R.J.N., Dhalla, N., Guin, R., Hirst, C., Hirst, M., Holt, R.A., Lee, D., Li, H.I., Mayo, M., Moore, R.A., Schein, J.E., Slobodan, J.R., Tam, A., Thiessen,

N., Varhol, R., Zeng, T., Zhao, Y., Jones, S.J.M., Marra, M.A., Bass, A.J., Ramos, A.H., Cherniack, A.D., Schumacher, S.E., Tabak, B., Carter, S.L., Pho, N.H., Nguyen, H., Onofrio, R.C., Crenshaw, A., Ardlie, K., Beroukhim, R., Winckler, W., Meyerson, M., Protopopov, A., Zhang, J., Hadjipanayis, A., Lee, E., Xi, R., Yang, L., Ren, X., Sathiamoorthy, N., Chen, P.-C., Haseley, P., Xiao, Y., Lee, S., Seidman, J., Kucherlapati, R., Todd Auman, J., Hoadley, K.A., Du, Y., Wilkerson, M.D., Shi, Y., Liquori, C., Meng, S., Li, L., Turman, Y.J., Topal, M.D., Tan, D., Waring, S., Buda, E., Walsh, J., Jones, C.D., Mieczkowski, P.A., Singh, D., Wu, J., Gulabani, A., Dolina, P., Bodenheimer, T., Hoyle, A.P., Simons, J.V., Soloway, M., Mose, L.E., Jefferys, S.R., Balu, S., O'Connor, B.D., Prins, J.F., Chiang, D.Y., Neil Hayes, D., Perou, C.M., Hinoue, T., Weisenberger, D.J., Maglinte, D.T., Pan, F., Berman, B.P., Van Den Berg, D.J., Shen, H., Triche, T., Jr, Baylin, S.B., Laird, P.W., Getz, G., Noble, M., Voet, D., Saksena, G., Gehlenborg, N., DiCara, D., Zhang, H., Wu, C.-J., Yingchun Liu, S., Shukla, S., Lawrence, M.S., Zhou, L., Sivachenko, A., Lin, P., Jing, R., Park, R.W., Nazaire, M.-D., Robinson, J., Thorvaldsdottir, H., Mesirov, J., Park, P.J., Chin, L., Thorsson, V., Reynolds, S.M., Bernard, B., Kreisberg, R., Lin, J., Iype, L., Bressler, R., Erkkilä, T., Gundapuneni, M., Liu, Y., Norberg, A., Robinson, T., Yang, D., Zhang, W., Shmulevich, I., de Ronde, J.J., Schultz, N., Cerami, E., Ciriello, G., Goldberg, A.P., Gross, B., Jacobsen, A., Gao, J., Kaczkowski, B., Sinha, R., Arman Aksoy, B., Antipin, Y., Reva, B., Shen, R., Taylor, B.S., Ladanyi, M., Sander, C., Akbani, R., Zhang, N., Broom, B.M., Casasent, T., Unruh, A., Wakefield, C., Hamilton, S.R., Craig Cason, R., Baggerly, K.A., Weinstein, J.N., Haussler, D., Benz, C.C., Stuart, J.M., Benz, S.C., Zachary Sanborn, J., Vaske, C.J., Zhu, J., Szeto, C., Scott, G.K., Yau, C., Ng, S., Goldstein, T., Ellrott, K., Collisson, E., Cozen, A.E., Zerbino, D., Wilks, C., Craft, B., Spellman, P., Penny, R., Shelton, T., Hatfield, M., Morris, S., Yena, P., Shelton, C., Sherman, M., Paulauskis, J., Gastier-Foster, J.M., Bowen, J., Ramirez, N.C., Black, A., Pyatt, R., Wise, L., White, P., Bertagnolli, M., Brown, J., Chan, T.A., Chu, G.C., Czerwinski, C., Denstman, F., Dhir, R., Dörner, A., Fuchs, C.S., Guillem, J.G., Iacocca, M., Juhl, H., Kaufman, A., Kohl, B., III, Van Le, X., Mariano, M.C., Medina, E.N., Meyers, M., Nash, G.M., Paty, P.B., Petrelli, N., Rabeno, B., Richards, W.G., Solit, D., Swanson, P., Temple, L., Tepper, J.E., Thorp, R., Vakiani, E., Weiser, M.R., Willis, J.E., Witkin, G., Zeng, Z., Zinner, M.J., Zornig, C., Jensen, M.A., Sfeir, R., Kahn, A.B., Chu, A.L., Kothiyal, P., Wang, Z., Snyder, E.E., Pontius, J., Pihl, T.D., Ayala, B., Backus, M., Walton, J., Whitmore, J., Baboud, J., Berton, D.L., Nicholls, M.C., Srinivasan, D., Raman, R., Girshik, S., Kigonya, P.A., Alonso, S., Sanbhadti, R.N., Barletta, S.P., Greene, J.M., Pot, D.A., Mills Shaw, K.R., Dillon, L.A.L., Buetow, K., Davidsen, T., Demchok, J.A., Eley, G., Ferguson, M., Fielding, P., Schaefer, C., Sheth, M., Yang, L., Guyer, M.S., Ozenberger, B.A., Palchik, J.D., Peterson, J., Sofia, H.J., Thomson, E., 2012. Comprehensive molecular characterization of human colon and rectal cancer. Nature 487, 330–337. doi:10.1038/nature11252

Oudhoff, M.J., Freeman, S.A., Couzens, A.L., Antignano, F., Kuznetsova, E., Min, P.H., Northrop, J.P., Lehnertz, B., Barsyte-Lovejoy, D., Vedadi, M., Arrowsmith, C.H., Nishina, H., Gold, M.R., Rossi, F.M.V., Gingras, A.-C., Zaph, C., 2013. Control of the hippo pathway by Set7-dependent methylation of Yap. Dev Cell 26, 188–194. doi:10.1016/j.devcel.2013.05.025

Park, H.W., Kim, Y.C., Yu, B., Moroishi, T., Mo, J.-S., Plouffe, S.W., Meng, Z., Lin,

K.C., Yu, F.-X., Alexander, C.M., Wang, C.-Y., Guan, K.-L., 2015. Alternative Wnt Signaling Activates YAP/TAZ. Cell 162, 780–794. doi:10.1016/j.cell.2015.07.013
Pokutta, S., Weis, W.I., 2000. Structure of the dimerization and beta-catenin-binding region of alpha-catenin. Mol Cell 5, 533–543.
Powell, A.E., Wang, Y., Li, Y., Poulin, E.J., Means, A.L., Washington, M.K., Higginbotham, J.N., Juchheim, A., Prasad, N., Levy, S.E., Guo, Y., Shyr, Y., Aronow, B.J., Haigis, K.M., Franklin, J.L., Coffey, R.J., 2012. The pan-ErbB negative regulator Lrig1 is an intestinal stem cell marker that functions as a tumor suppressor. Cell 149, 146–158. doi:10.1016/j.cell.2012.02.042
Rosenbluh, J., Nijhawan, D., Cox, A.G., Li, X., Neal, J.T., Schafer, E.J., Zack, T.I., Wang, X., Tsherniak, A., Schinzel, A.C., Shao, D.D., Schumacher, S.E., Weir, B.A., Vazquez, F., Cowley, G.S., Root, D.E., Mesirov, J.P., Beroukhim, R., Kuo, C.J., Goessling, W., Hahn, W.C., 2012. β-Catenin-driven cancers require a YAP1 transcriptional complex for survival and tumorigenesis. Cell 151, 1457–1473. doi:10.1016/j.cell.2012.11.026
Sangiorgi, E., Capecchi, M.R., 2008. Bmi1 is expressed in vivo in intestinal stem cells. Nat Genet 40, 915–920. doi:10.1038/ng.165
Sansom, O.J., Meniel, V.S., Muncan, V., Phesse, T.J., Wilkins, J.A., Reed, K.R., Vass, J.K., Athineos, D., Clevers, H., Clarke, A.R., 2007. Myc deletion rescues Apc deficiency in the small intestine. Nature 446, 676–679. doi:10.1038/nature05674
Sato, T., Clevers, H., 2013. Primary mouse small intestinal epithelial cell cultures. Methods Mol. Biol. 945, 319–328. doi:10.1007/978-1-62703-125-7_19
Sato, T., Vries, R.G., Snippert, H.J., van de Wetering, M., Barker, N., Stange, D.E., van Es, J.H., Abo, A., Kujala, P., Peters, P.J., Clevers, H., 2009. Single Lgr5 stem cells build crypt-villus structures in vitro without a mesenchymal niche. Nature 459, 262–265. doi:10.1038/nature07935
Schlegelmilch, K., Mohseni, M., Kirak, O., Pruszak, J., Rodriguez, J.R., Zhou, D., Kreger, B.T., Vasioukhin, V., Avruch, J., Brummelkamp, T.R., Camargo, F.D., 2011. Yap1 Acts Downstream of α-Catenin to Control Epidermal Proliferation. Cell 144, 782–795. doi:10.1016/j.cell.2011.02.031
Schmitz, Y., Rateitschak, K., Wolkenhauer, O., 2013. Analysing the impact of nucleo-cytoplasmic shuttling of β-catenin and its antagonists APC, Axin and GSK3 on Wnt/β-catenin signalling. Cellular Signalling 25, 2210–2221. doi:10.1016/j.cellsig.2013.07.005
Schwitalla, S., Fingerle, A.A., Cammareri, P., Nebelsiek, T., Göktuna, S.I., Ziegler, P.K., Canli, O., Heijmans, J., Huels, D.J., Moreaux, G., Rupec, R.A., Gerhard, M., Schmid, R., Barker, N., Clevers, H., Lang, R., Neumann, J., Kirchner, T., Taketo, M.M., van den Brink, G.R., Sansom, O.J., Arkan, M.C., Greten, F.R., 2013. Intestinal tumorigenesis initiated by dedifferentiation and acquisition of stem-cell-like properties. Cell 152, 25–38. doi:10.1016/j.cell.2012.12.012
Shen, C., Wang, D., Liu, X., Gu, B., Du, Y., Wei, F.-Z., Cao, L.-L., Song, B., Lu, X., Yang, Q., Zhu, Q., Hou, T., Li, M., Wang, L., Wang, H., Zhao, Y., Yang, Y., Zhu, W.-G., 2015. SET7/9 regulates cancer cell proliferation by influencing β-catenin stability. Faseb J. doi:10.1096/fj.15-273540
Silvis, M.R., Kreger, B.T., Lien, W.-H., Klezovitch, O., Rudakova, G.M., Camargo, F.D., Lantz, D.M., Seykora, J.T., Vasioukhin, V., 2011. α-catenin is a tumor suppressor that controls cell accumulation by regulating the localization and activity of the

transcriptional coactivator Yap1. Sci Signal 4, ra33–ra33. doi:10.1126/scisignal.2001823
Stewart, B.W., Wild, C.P., 2014. World Cancer Report 2014. World Health Organization.
Takeda, N., Jain, R., LeBoeuf, M.R., Wang, Q., Lu, M.M., Epstein, J.A., 2011. Interconversion Between Intestinal Stem Cell Populations in Distinct Niches. Science 334, 1420–1424. doi:10.1126/science.1213214
Tanaka, T., Kohno, H., Suzuki, R., Hata, K., Sugie, S., Niho, N., Sakano, K., Takahashi, M., Wakabayashi, K., 2006. Dextran sodium sulfate strongly promotes colorectal carcinogenesis in Apc(Min/+) mice: inflammatory stimuli by dextran sodium sulfate results in development of multiple colonic neoplasms. International journal of cancer. Journal international du cancer 118, 25–34. doi:10.1002/ijc.21282
Tetteh, P.W., Basak, O., Farin, H.F., Wiebrands, K., Kretzschmar, K., Begthel, H., van den Born, M., Korving, J., de Sauvage, F., van Es, J.H., van Oudenaarden, A., Clevers, H., 2016. Replacement of Lost Lgr5-Positive Stem Cells through Plasticity of Their Enterocyte-Lineage Daughters. Cell Stem Cell 18, 203–213. doi:10.1016/j.stem.2016.01.001
Tetteh, P.W., Farin, H.F., Clevers, H., 2015. Plasticity within stem cell hierarchies in mammalian epithelia. Trends Cell Biol. 25, 100–108. doi:10.1016/j.tcb.2014.09.003
Tian, H., Biehs, B., Warming, S., Leong, K.G., Rangell, L., Klein, O.D., de Sauvage, F.J., 2011. A reserve stem cell population in small intestine renders Lgr5-positive cells dispensable. Nature 478, 255–259. doi:10.1038/nature10408
van der Flier, L.G., van Gijn, M.E., Hatzis, P., Kujala, P., Haegebarth, A., Stange, D.E., Begthel, H., van den Born, M., Guryev, V., Oving, I., van Es, J.H., Barker, N., Peters, P.J., van de Wetering, M., Clevers, H., 2009. Transcription Factor Achaete Scute-Like 2 Controls Intestinal Stem Cell Fate. Cell 136, 903–912. doi:10.1016/j.cell.2009.01.031
van Es, J.H., Sato, T., van de Wetering, M., Lyubimova, A., Yee Nee, A.N., Gregorieff, A., Sasaki, N., Zeinstra, L., van den Born, M., Korving, J., Martens, A.C.M., Barker, N., van Oudenaarden, A., Clevers, H., 2012. Dll1+ secretory progenitor cells revert to stem cells upon crypt damage. Nat Cell Biol 14, 1099–1104. doi:10.1038/ncb2581
Varelas, X., Miller, B.W., Sopko, R., Song, S., Gregorieff, A., Fellouse, F.A., Sakuma, R., Pawson, T., Hunziker, W., McNeill, H., 2010. The Hippo pathway regulates Wnt/beta-catenin signaling. Dev Cell 18, 579–591. doi:10.1016/j.devcel.2010.03.007
Vermeulen, L., Snippert, H.J., 2014. Stem cell dynamics in homeostasis and cancer of the intestine. Nature Publishing Group 14, 468–480. doi:10.1038/nrc3744
Vogelstein, B., Papadopoulos, N., Velculescu, V.E., Zhou, S., Diaz, L.A., Kinzler, K.W., 2013. Cancer genome landscapes. Science 339, 1546–1558. doi:10.1126/science.1235122
Wada, K.-I., Itoga, K., Okano, T., Yonemura, S., Sasaki, H., 2011. Hippo pathway regulation by cell morphology and stress fibers. Development 138, 3907–3914. doi:10.1242/dev.070987
Yan, Y., Kolachala, V., Dalmasso, G., Nguyen, H., Laroui, H., Sitaraman, S.V., Merlin, D., 2009. Temporal and spatial analysis of clinical and molecular parameters in dextran sodium sulfate induced colitis. PLoS One 4, e6073. doi:10.1371/journal.pone.0006073
Zeng, L., Fagotto, F., Zhang, T., Hsu, W., Vasicek, T.J., Perry, W.L., Lee, J.J., Tilghman, S.M., Gumbiner, B.M., Costantini, F., 1997. The mouse Fused locus encodes Axin,

an inhibitor of the Wnt signaling pathway that regulates embryonic axis formation. Cell 90, 181–192.

Zhou, D., Zhang, Y., Wu, H., Barry, E., Yin, Y., Lawrence, E., Dawson, D., Willis, J.E., Markowitz, S.D., Camargo, F.D., Avruch, J., 2011. Mst1 and Mst2 protein kinases restrain intestinal stem cell proliferation and colonic tumorigenesis by inhibition of Yes-associated protein (Yap) overabundance. Proc Natl Acad Sci U S A 108, E1312–20. doi:10.1073/pnas.1110428108

FIGURE LEGENDS

Figure 1. SETD7 is required for Wnt-mediated tumorigenesis

A, Kaplan-Meier curve of *Apc*$^{Min/+}$ / *Setd7*$^{+/-}$ and *Apc*$^{Min/+}$ / *Setd7*$^{-/-}$ female mice (n>11). **B,** Number of tumors found in the small intestines of female mice indicated at endpoint. (n>15) A small group of aged males were assessed separately (Figure S1A). **C,** Number of tumors found in the colons of mice indicated in (B). **D,** Number of tumors found in the colons of indicated male mice 4 weeks after DSS treatment (7 days, 2.5%). n>8, pooled from 2 independent experiments. **E,** Gene expression analysis of small intestinal tumors (n>7 mice) of indicated mice compared to normal adjacent tissue. A small set of other relevant genes can be found in Figure S1B. **F & G,** Staining for β-Catenin of small intestinal tumors from aged mice. **H,** Lysozyme staining marking Paneth cells in small intestinal tumors from aged mice. **I,** Gene expression analysis of *Apc*^{Min}-tumor derived organoids that were treated with SETD7 inhibitor (*R*)-PFI-2 for 48 hours (n>7, from 2 independent experiments). * P<0.05, ** P<0.01, *** P<0.001

Figure 2. IEC-intrinsic expression of *Setd7* is required for regeneration after DSS-induced damage

A, Weight loss in *Setd7*$^{f/f}$ (black) and *Setd7*$^{\Delta IEC}$ (grey) mice following 5 days of 3.5% (w/v) DSS treatment. n>7. **B,** H&E stained colonic sections were quantified for indications of pathology (infiltrating immune cells, crypt repair, muscle thickness). **C,** H&E staining of distal colon (day 15). Black arrows indicate crypt invagination/fission. **D,** Gene expression analysis of isolated IECs isolated at days 7/8 from *Setd7*$^{f/f}$ (black) and *Setd7*$^{\Delta IEC}$ (grey) mice. n>7. * P<0.05, ** P<0.01, *** P<0.001.

Figure 3. IEC-intrinsic expression of *Setd7* is required for regeneration after irradiation-induced damage and organoid formation

A & B H&E staining of small intestinal sections 3 and 6 days after lethal irradiation (10 Gy). **C,** Crypts counted from sections as shown in A&B. Mice in each group; d0=3, d3=4, d6=6. *Setd7*$^{f/f}$ (black) and *Setd7*$^{\Delta IEC}$ (grey). **D,** Gene expression analysis of IECs during regeneration (days 6 and 7). *Setd7*$^{f/f}$ (black) and *Setd7*$^{\Delta IEC}$ (grey). n>9 pooled from 3 independent experiments. *** P<0.001. **E,** Organoid efficiency as calculated from images

such as Figure S3A. **F,** Intestinal organoids generated from crypts isolated from *Setd7*$^{+/-}$ or *Setd7*$^{-/-}$ mice from day 1 to 5. **G,** Gene expression analysis of organoid cultures from *Setd7*$^{+/-}$ (black) or *Setd7*$^{-/-}$ (white) mice. n>5 from 2 independent crypt isolations. **H,** Gene expression from organoids derived from C57BL/6 mice treated with (*R*)-PFI-2 (1 μM) for 72 h. n=6 from 2 independent experiments. * P<0.05, ** P<0.01 *** P<0.001.

Figure 4. SETD7 does not affect intestinal homeostasis

A, H&E staining of naïve small intestines from indicated mice. **B,** IECs from small intestines of naïve *Setd7*$^{f/f}$ (black) or *Setd7*$^{\Delta IEC}$ (grey) mice were isolated and gene expression of indicated genes was assessed by qPCR. Relative expression is fold over *Setd7*$^{f/f}$ mice, using *Actb* as housekeeping gene. n=10, pooled from 3 separate IEC preparations. **C,** Flow cytometry of DAPI-negative gated crypt IECs using endogenous GFP, from *Lgr5*^{EGFP}*/Setd7*$^{+/-}$ and *Lgr5*^{EGFP}*/Setd7*$^{-/-}$ mice. Mean ± SD is indicated, n=5. **D,** Organoid efficiency from single sorted Lgr5^{high} cells (sorted as shown in **C**).

Figure 5. SETD7 is required for Wnt signaling *in vitro* by mediating nuclear accumulation of β-Catenin

A, Expression of β-Catenin (β-Cat), SETD7 and GAPDH in HEK293 cells at 0, 0.5, 1, 2 and 4 hours following treatment with Wnt3A in the presence of (*R*)-PFI-2 or its negative enantiomer (*S*)-PFI-2 was analyzed by western blot. **B,** *AXIN2* expression analyzed by qPCR after 4 hours of Wnt3A with (*S*)-PFI-2 (*S*) or (*R*)-PFI-2 (*R*). **C,** HEK293 protein levels upon LiCl (20 mM) treatment was assessed by western blot. **D,** *AXIN2* expression analyzed by qPCR following incubation for 4 h with LiCl (20 mM). **E,** Expression of β-Catenin (β-Cat), in cytosolic (cyto.) or nuclear (nucl.) fractions from HEK293 cells at 0, 2 and 4 hours following treatment with CHIR in the presence of (*R*)-PFI-2 or (*S*)-PFI-2 was analyzed by western blot. **F,** Cytosolic β-Catenin as calculated from images as shown (E), β-Catenin / GAPDH relative levels are shown. N=3 **G,** Nuclear β-Catenin as calculated from images as shown (E). Nuclear β-Catenin accumulation was calculated compared β-Catenin at t= 0. N=4 **H & I,** Nuclear accumulation of β-Catenin in HEK293 cells was visualized by confocal microscopy at 4h post-Wnt3A treatment (H) and quantified at 0, 0.5, 2 and 4 hours post-Wnt3A treatment (I). **J,** HEK293 cells were

treated with Wnt3A (4 h) and (*R*)-PFI-2 or (*S*)-PFI-2 was added 0.5, 1 and 2 hours before fixation. Nuclear accumulation of β-Catenin was visualized by confocal microscopy and quantified 4 hours post-Wnt3A treatment. * P<0.05, ** P<0.01, *** P<0.001

Figure 6. SETD7-dependent regulation of Wnt signaling requires YAP

A, Western blots of HEK293 protein levels using indicated antibodies. Knockdown of *SETD7* (S7, pooled '1' and '2'), *YAP* (also 2 constructs pooled), or both (*S7&YAP*) in cells that were treated with LiCl (20 mM) for 4 h. **B,** LiCl-induced expression of *AXIN2* and *CTGF* following siRNA-mediated knockdown of *SETD7* (S7), *YAP* (Y) or both (Y/S7) in HEK293 cells was analyzed by qPCR. **C,** Inputs and anti-MYC immunoprecipitates (IP) from HEK293 cells expressing MYC-AXIN1 and HA-SETD7 were immunoblotted with anti-AXIN1, anti-SETD7 and anti-GAPDH antibodies. **D,** Inputs and anti-β-Catenin IP from HEK293 cells treated with (*S*)-PFI2 (*S*) or (*R*)-PFI-2 (*R*). HC is the heavy chain of the anti-β-Catenin antibody used for IP, band below HC is SETD7. **E,** Inputs and anti-SETD7 immunoprecipitates from HEK293 cells treated with (*S*)-PFI2 (*S*) or (*R*)-PFI-2 (*R*) in the absence or presence of Wnt3A were immunoblotted with anti-SETD7 and anti-β-Catenin antibodies. **F,** Inputs and anti-YAP IP from HEK293 cells treated with (*S*)-PFI2 (*S*) or (*R*)-PFI-2 (*R*) were immunoblotted with anti-YAP and anti-β-Catenin antibodies. **G,** Inputs and anti-YAP IP from HEK293 cells treated with CHIR and/or (*R*)-PFI-2 (*R*) for 2 h were immunoblotted with anti-YAP and anti-β-Catenin antibodies. **H,** Inputs and anti-YAP IP from HEK293 cells treated with (*S*)-PFI2 (*S*) or (*R*)-PFI-2 (*R*) for 2 h were immunoblotted with anti-YAP and anti-AXIN1 antibodies. **I,** Inputs and anti-FLAG immunoprecipitates (IP) from HEK293 cells expressing MYC-AXIN1 and FLAG-YAP^{K494R}, FLAG-YAP^{K497R}, and FLAG-YAP^{2KR} were immunoblotted with anti-AXIN1, anti-FLAG antibodies. **G,** Organoids derived from indicated genotypes were treated with Verteporfin (3 μM) for 5 days. **H**, Gene expression from organoids as described in (G) of *Setd7*$^{+/-}$ (black bars) and *Setd7*$^{-/-}$ (white bars). n=4 from 2 independent experiments. * P<0.05, *** P<0.001.

Figure 7. Cell density regulates SETD7 localization, which is important for its control of the Wnt pathway

A, YAP and SETD7 localization in sparse or dense HEK293 cultures was assessed by confocal imaging. **B,** SETD7 localization under sparse and dense conditions in Caco-2 and MCF7 cell lines. **C,** *AXIN2* expression was assessed by qPCR in control and LiCl-treated HEK293 cells under sparse conditions. 'C' is siControl and S7 is pooled si*SETD7_1* and *siSETD7_2* as used in Figures 5 and 6. n=6, pooled from 3 n=2 experiments. * P<0.05. **D,** Immunohistochemistry of SETD7 in mouse intestinal crypts, $Apc^{Min/+}$ derived tumor, and from $Setd7^{-/-}$ tissue as control for the antibody.

1 **Figure 1.**

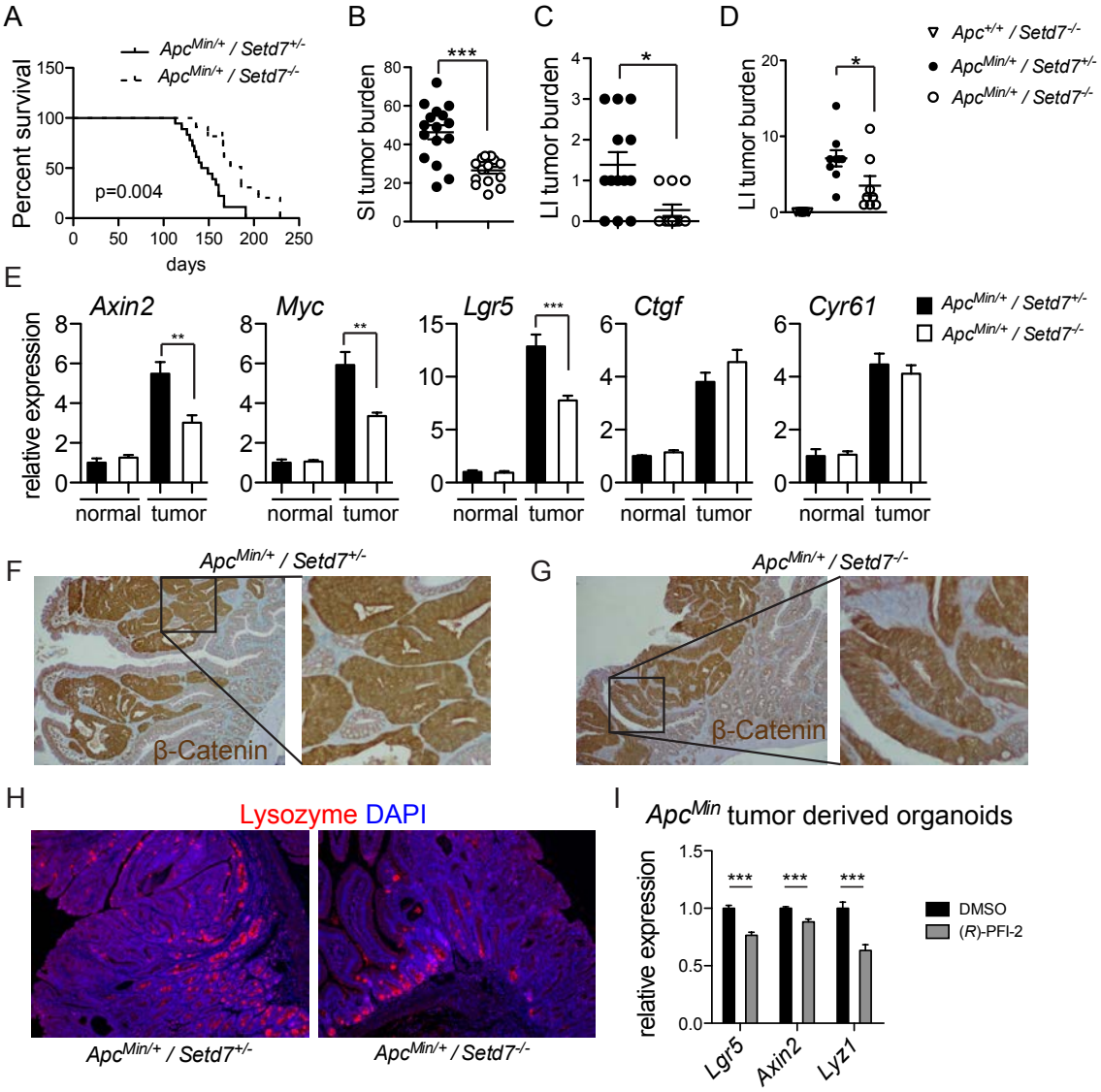
A
Apc^Min/+ / Setd7^+/-
Apc^Min/+ / Setd7^-/-
Percent survival
p=0.004
days
B
SI tumor burden
C
LI tumor burden
D
LI tumor burden
Apc^+/+ / Setd7^-/-
Apc^Min/+ / Setd7^+/-
Apc^Min/+ / Setd7^-/-
E
Axin2
Myc
Lgr5
Ctgf
Cyr61
relative expression
normal
tumor
F
Apc^Min/+ / Setd7^+/-
β-Catenin
G
Apc^Min/+ / Setd7^-/-
β-Catenin
H
Lysozyme DAPI
Apc^Min/+ / Setd7^+/-
Apc^Min/+ / Setd7^-/-
I
Apc^Min tumor derived organoids
relative expression
DMSO
(R)-PFI-2
Lgr5
Axin2
Lyz1

Figure 2.

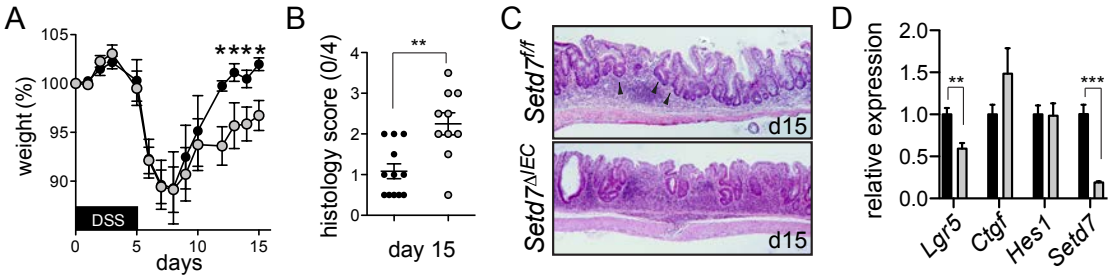
A
105
100
95
90
weight (%)
DSS
0
5
10
15
days
****
B
histology score (0/4)
4
3
2
1
0
**
day 15
C
Setd7f/f
Setd7ΔIEC
d15
d15
D
relative expression
2.0
1.5
1.0
0.5
0.0
**
***
Lgr5
Ctgf
Hes1
Setd7

Figure 3.

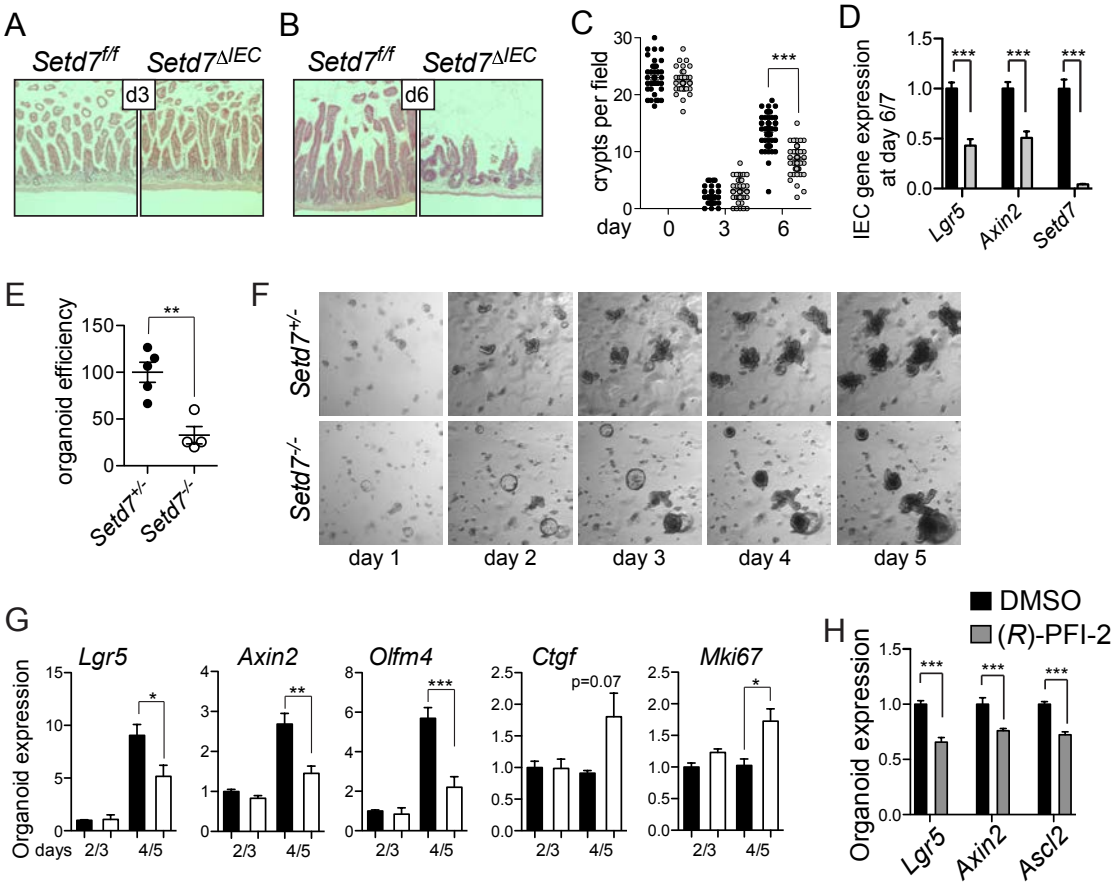
A
Setd7f/f
Setd7ΔIEC
d3
B
Setd7f/f
Setd7ΔIEC
d6
C
crypts per field
day
0
3
6
***
D
IEC gene expression at day 6/7
***
***
***
Lgr5
Axin2
Setd7
E
organoid efficiency
**
Setd7+/-
Setd7-/-
F
Setd7+/-
Setd7-/-
day 1
day 2
day 3
day 4
day 5
G
Lgr5
Axin2
Olfm4
Ctgf
p=0.07
Mki67
Organoid expression
days
2/3
4/5
H
DMSO
(R)-PFI-2
Organoid expression
Lgr5
Axin2
Ascl2

Figure 4.

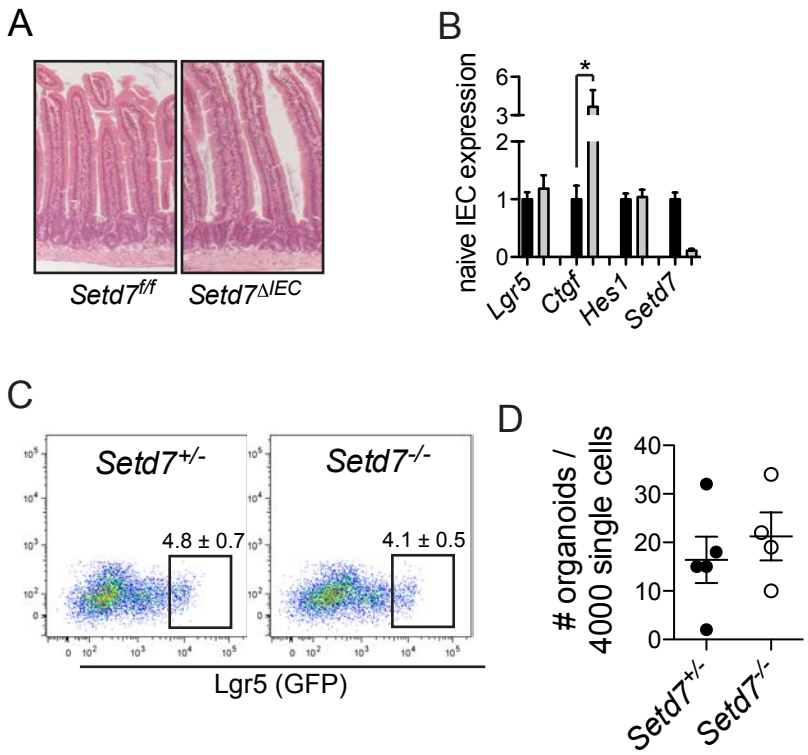
A
Setd7f/f
Setd7ΔIEC
B
naive IEC expression
6
3
2
1
0
*
Lgr5
Ctgf
Hes1
Setd7
C
Setd7+/-
4.8 ± 0.7
Setd7-/-
4.1 ± 0.5
Lgr5 (GFP)
D
organoids / 4000 single cells
40
30
20
10
0
Setd7+/-
Setd7-/-

Figure 5.

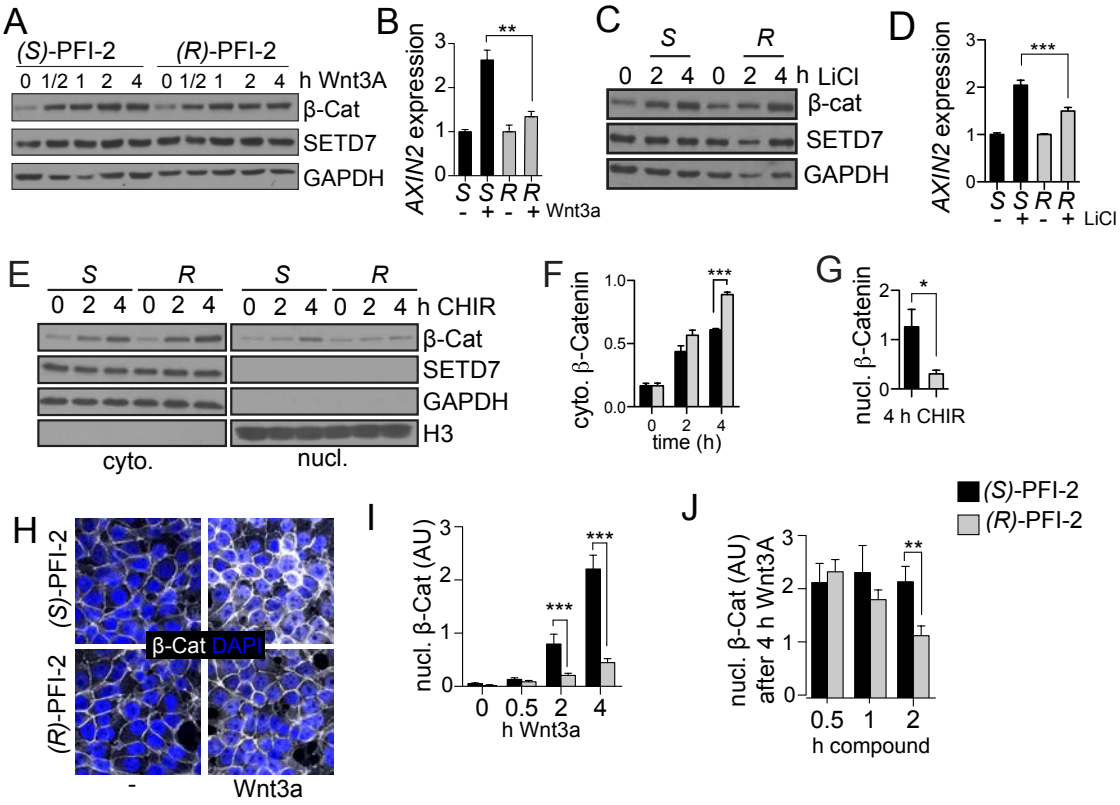
A
(S)-PFI-2
(R)-PFI-2
0 1/2 1 2 4 0 1/2 1 2 4 h Wnt3A
β-Cat
SETD7
GAPDH
B
AXIN2 expression
S S R R
- + - + Wnt3a
C
S R
0 2 4 0 2 4 h LiCl
β-cat
SETD7
GAPDH
D
AXIN2 expression
S S R R
- + - + LiCl
E
S R S R
0 2 4 0 2 4 0 2 4 0 2 4 h CHIR
β-Cat
SETD7
GAPDH
H3
cyto.
nucl.
F
cyto. β-Catenin
time (h)
G
nucl. β-Catenin
4 h CHIR
H
(S)-PFI-2
(R)-PFI-2
β-Cat DAPI
-
Wnt3a
I
nucl. β-Cat (AU)
h Wnt3a
J
(S)-PFI-2
(R)-PFI-2
nucl. β-Cat (AU) after 4 h Wnt3A
h compound

Figure 6.

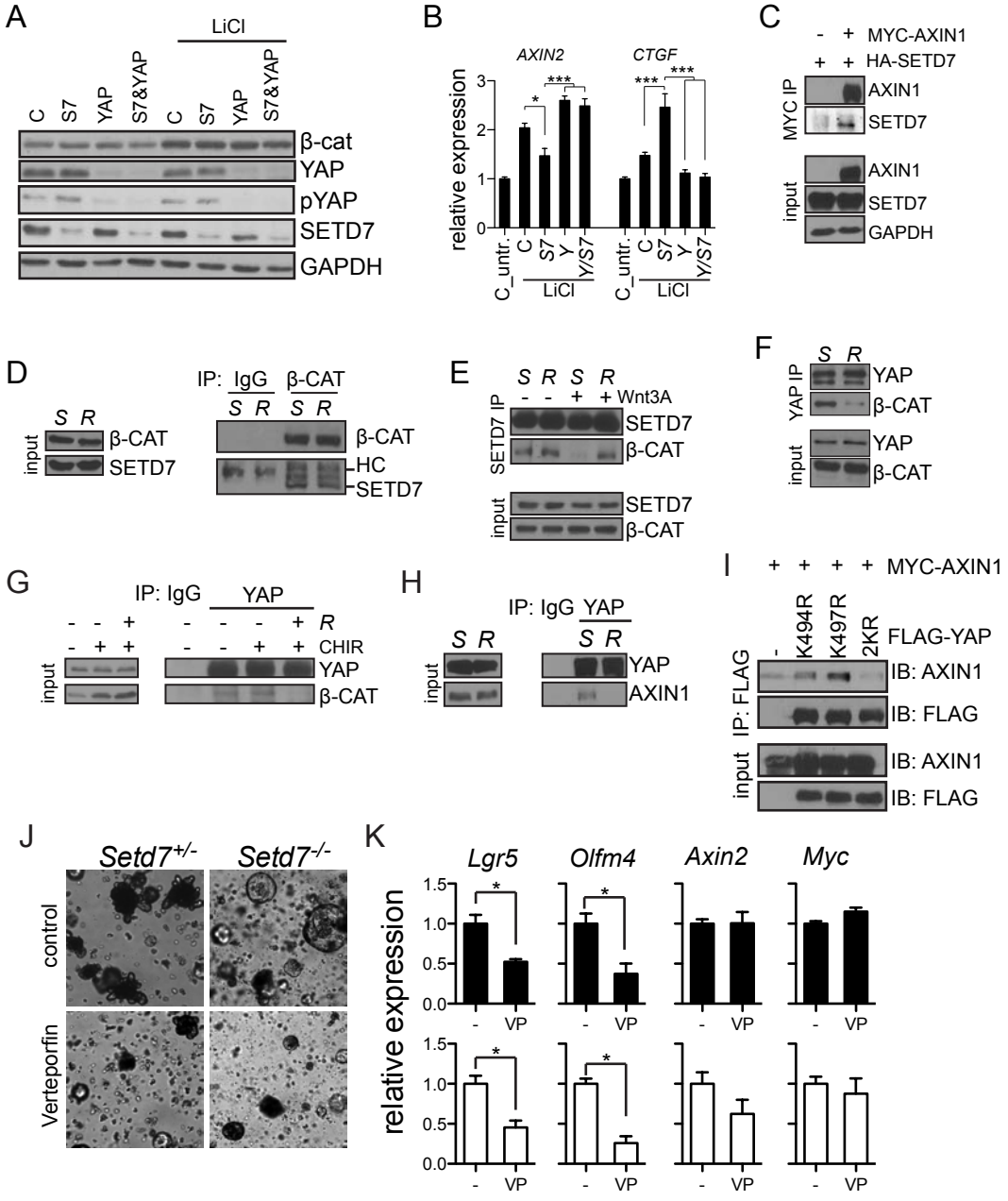
A
LiCl
C
S7
YAP
S7&YAP
β-cat
YAP
pYAP
SETD7
GAPDH
B
AXIN2
CTGF
relative expression
C_untr.
LiCl
C
S7
Y
Y/S7
C
MYC-AXIN1
HA-SETD7
MYC IP
AXIN1
SETD7
input
GAPDH
D
IP: IgG β-CAT
S R S R
input
β-CAT
SETD7
HC
E
S R S R
Wnt3A
SETD7 IP
SETD7
β-CAT
F
YAP IP
YAP
β-CAT
G
IP: IgG YAP
CHIR
H
IP: IgG YAP
AXIN1
I
MYC-AXIN1
FLAG-YAP
K494R
K497R
2KR
IP: FLAG
IB: AXIN1
IB: FLAG
J
Setd7+/-
Setd7-/-
control
Verteporfin
K
Lgr5
Olfm4
Axin2
Myc
VP

Figure 7.

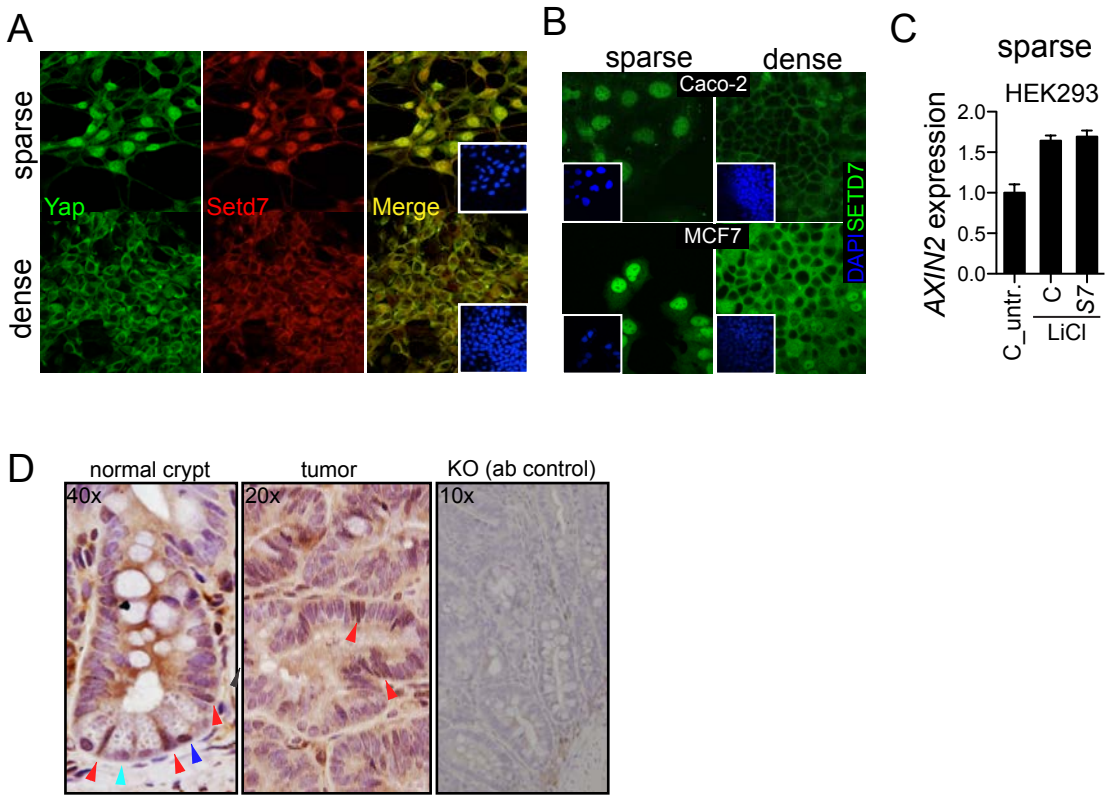
A
sparse
dense
Yap
Setd7
Merge
B
sparse
dense
Caco-2
MCF7
DAPI SETD7
C
sparse
HEK293
AXIN2 expression
2.0
1.5
1.0
0.5
0.0
C_untr.
C
S7
LiCl
D
normal crypt
tumor
KO (ab control)
40x
20x
10x